Neurobiology of Aging 72 (2018) 106–120

Contents lists available at ScienceDirect

Neurobiology of Aging

journal homepage: www.elsevier.com/locate/neuaging

Age-related differences in information processing during movie watching

Linda Geerligs [a,*], Cam-CAN [b], Karen L. Campbell [c]

[a] Donders Institute for Brain, Cognition and Behaviour, Radboud University, Nijmegen, the Netherlands
[b] Cambridge Centre for Ageing and Neuroscience (Cam-CAN), University of Cambridge and MRC Cognition and Brain Sciences Unit, Cambridge, UK
[c] Department of Psychology, Brock University, St. Catharines, Canada

ARTICLE INFO

Article history:
Received 5 March 2018
Received in revised form 27 July 2018
Accepted 29 July 2018
Available online 4 August 2018

Keywords:
Aging
Functional connectivity
Naturalistic viewing
Intersubject correlation
Dynamics
Attentional control
fMRI
Language
Memory

ABSTRACT

We know how age affects the brain during lab-based tasks, but what about situations truer to everyday life, such as watching movies? We measured functional magnetic resonance imaging activity while participants (N = 577) from the Cambridge Centre for Ageing and Neuroscience (www.cam-can.com) watched a movie. Watching the same movie induces significant intersubject synchronization of brain activity across participants. These cross-subject correlations suggest that viewers are processing incoming information in a similar (or shared) way. We show that with advancing age, synchrony is preserved in some areas, including the language network, but decreased in others, including the medial prefrontal cortex, medial temporal lobe, and fronto-parietal network. Synchrony declines were driven by more idiosyncratic responding in older adults and were associated with regionally distinct temporal profiles and functional connectivity patterns, as well as declines in white matter integrity. These findings suggest that areas involved in language processing remain intact with age, while regions involved in attentional control and memory may show age-related declines, even in situations similar to daily life.

1. Introduction

The seeming contradiction of neurocognitive aging research is that age is associated with decreased performance on a number of lab-based tasks, and yet in daily life, most healthy older adults are able to function quite well (Zimmerman et al., 2011). They read books, watch movies, socialize with friends and family—rarely complaining that they are unable to understand language, process meaning, or experience emotions. This raises the question of how age-related declines in functions like attentional control and memory observed in the lab affect the processing of more naturalistic stimuli, such as movies. Movies offer rich and complex stimulation, which more closely approximate everyday life relative to the highly constrained visual and auditory stimuli that are used in most experiments; this is why they are referred to as naturalistic stimuli (Hasson et al., 2004). On the one hand, we might expect minimal age differences in the processing of these stimuli, in that narrative comprehension taps into one's existing body of knowledge which is, if anything, more extensive in older adults (for a recent review, see Umanath and Marsh, 2014). Moreover, most movies tend to be rich with emotion, and previous work has shown that increasing the emotional meaningfulness of stimuli can reduce age differences in attention and memory (Mather and Carstensen, 2005; May et al., 2005). On the other hand, movie watching requires sustained attentional control (Naci et al., 2014) and ongoing retrieval from and encoding to memory (Hasson et al., 2015), processes which are known to decline with age (Craik and Byrd, 1982). These processes depend on networks (such as the frontoparietal control and default network) that are negatively affected by age (e.g., Campbell et al., 2012; Damoiseaux et al., 2008; Grady et al., 2010; Turner and Spreng, 2015). Thus, we might expect age to affect the processing of movies and this has been shown in some behavioral work (Kurby and Zacks, 2011; Zacks et al., 2006), however also see Kurby et al. (2014).

At a neural level, movies have been shown to drive activation in a similar way across participants. In young adults, these cross-subject correlations (or synchronous responses) in the functional magnetic resonance imaging (fMRI) blood oxygenation level dependent (BOLD) signal have been associated with intact processing (Hasson et al., 2009) and more similarity in information processing across individuals (Naci et al., 2014). Cross-subject

* Corresponding author at: Donders Institute for Brain, Cognition and Behaviour, Montessorilaan 3, Nijmegen 6525 HR, The Netherlands. Tel.: +31 243616091; fax: +31 24 3616066.
E-mail address: lindageerligs@gmail.com (L. Geerligs).

0197-4580/$ – see front matter © 2018 Published by Elsevier Inc.
https://doi.org/10.1016/j.neurobiolaging.2018.07.025

correlations not only tend to be strongest in primary auditory and visual regions but also extend to association cortex (including frontoparietal and medial frontal regions). Synchrony in these latter regions tends to be greatest when the stimulus itself is particularly captivating, presumably because viewers are attending to the same thing in each scene (Dmochowski et al., 2012; Dorr et al., 2010). Furthermore, synchrony in higher-order regions is observed when movies are presented in temporal order and at longer timescales (e.g., sentences, paragraphs) rather than cut up into constituent parts (e.g., words, syllables; Hasson et al., 2008). Presumably, this occurs because mental models of the narrative are built up gradually over time, primarily within a core network of regions including the medial prefrontal cortex (mPFC) and hippocampus (Simony et al., 2016; Van Kesteren et al., 2012).

In a recent preliminary study, we showed that neural synchrony declines with age during naturalistic viewing (Campbell et al., 2015). Using a subset of participants (N = 218) from the Cambridge Centre for Ageing and Neuroscience (Cam-CAN) project, we used independent components analysis to identify networks active during movie watching (i.e., while participants watched an 8-minute long Alfred Hitchcock movie in the fMRI scanner). We showed that cross-subject network synchrony declines with age and relates to measures of attentional control obtained outside the scanner, suggesting that older adults do process naturalistic stimuli in a different way to younger adults. However, a number of questions remain. For instance, which brain regions show preserved information processing with age and which show the most pronounced differences, and what kind of processes do these regions subserve? Does the decline in synchrony relate to specific elements of the movie? And can we identify potential causes of this effect, such as age-related declines in functional or structural connectivity?

In the present article, we aim to investigate these questions in the larger Cam-CAN sample (N = 577). The richness of movie stimuli allows us to investigate many functional systems in the brain simultaneously, which would not have been possible if we had used simpler, well-controlled stimuli. To preface our results, synchrony was preserved with age in some regions, including parts of the language network, dorsal precuneus, and right temporoparietal junction (TPJ), suggesting that in these areas, information processing remains intact across the lifespan. Other regions showed significant age-related declines in synchrony, including the frontoparietal control network (FPCN), medial temporal lobes (MTLs; including the hippocampus), and mPFC—the FPCN critical for cognitive control (Vincent et al., 2008) and the latter regions responsible for memory, imagination, and internal mentation more broadly (Schacter et al., 2012).

In the remainder of the article, we combine functional, structural, and behavioral data with a number of innovative methods to explore the nature and potential causes of the observed age-effects in these 3 regions. First, we determine whether age differences in these higher-order regions can be explained by concomitant differences in primary auditory and visual processing regions (used here as a proxy for sensory loss). Second, we determine whether different cognitive functions (namely, fluid intelligence, explicit memory, and processing speed) differentially predict age-related declines in the FPCN, MTL, and mPFC. Third, we test whether unique subgroups of participants emerge with age (i.e., people who respond to the movie in the same way as each other but differently to others) or whether people are simply becoming more idiosyncratic with age. Fourth, we examine how synchrony in these regions changes throughout the movie and whether there are certain time points when age differences are most pronounced. Finally, we examine how individual differences in synchrony relate to brain-wide differences in functional connectivity (FC) and underlying white matter (WM) microstructure. Together, these analyses offer novel ways of investigating the age-related differences in brain function during naturalistic viewing and provide insights on the underlying mechanisms and behavioral consequences of age-related changes in brain function.

2. Material and methods

2.1. Participants

Six hundred forty-four participants (18–88 years old, M = 54.3, standard deviation [SD] = 18.46, 318 males and 326 females) were included in this study, from the population-based sample of the Cam-CAN. Of this initial sample, 577 participants were included in the main analyses of this article, due to various issues with data quality or preprocessing (for details on exclusion see Section 2.4). A subset of this sample was also part of our initial study on age-related differences in intersubject synchrony (Campbell et al., 2015). Participants were included if no brain abnormalities were detected and if they completed the full (f)MRI testing session. Participants scored 25 or higher on the mini mental state examination (Folstein et al., 1975), had no contraindications to MRI, had normal or corrected-to-normal vision and hearing, were native English speakers, and had no neurological disorders (Shafto et al., 2014). More information about the final sample is presented in Table 1. Ethical approval for the study was obtained from the Cambridgeshire 2 (now East of England–Cambridge Central) Research Ethics Committee. Participants gave written informed consent.

2.2. Movie

Participants were scanned (using fMRI) while they watched a shortened version of a black and white television drama by Alfred Hitchcock called “Bang! You’re Dead.” In previous studies, a longer version of this movie has been shown to elicit robust brain activity, synchronized across younger participants (Hasson et al., 2009). Because of time constraints, the full 25-minute episode was condensed to 8 minutes with the narrative of the episode preserved (Shafto et al., 2014). Participants were instructed to watch, listen, and pay attention to the movie (they were not aware of its title, and no participant reported having seen it before).

2.3. fMRI data and image acquisition

These data were collected as part of a more extensive scanning session in a 3T Siemens TIM Trio, with a 32-channel head coil. This scanning session consisted of structural scans, a resting state scan, an audio-visual task, and ended with movie watching, more details about the data collection can be found in Shafto et al. (2014). During the movie watching, 193 volumes were acquired, using a multiecho, T2*-weighted echo-planar imaging (EPI) sequence. Each volume contained 32 axial slices (acquired in descending order), with slice thickness of 3.7 mm and interslice gap of 20% (repetition time (TR) = 2470 ms; 5 echoes [echo time (TE) = 9.4 ms, 21.2 ms, 33 ms, 45 ms, 57 ms]; flip angle = 78°; field-of-view (FOV) = 192 mm × 192 mm; voxel size = 3 mm × 3 mm × 4.44 mm), the acquisition time was 8 minutes and 13 seconds.

A high-resolution (1 mm × 1 mm × 1 mm) T1-weighted Magnetization Prepared Rapid Gradient Echo image was also acquired, in addition to a T2-weighted structural image (voxel size 1 mm × 1 mm × 1 mm) using a sampling perfection with application-optimized contrasts using different flip angle evolution sequence. Diffusion-weighted images (DWIs) were acquired with a twice-refocused spin-echo sequence. Thirty diffusion gradient directions were obtained for each of 2 b-values: 1000 and 2000 s/mm^2,

Table 1
Participant demographics and mean cognitive performance per age decile

Decile	1	2	3	4	5	6	7
Age range	18–27	28–37	38–47	48–57	58–67	68–77	78–88
N	47	98	94	90	86	83	79
Male/female	21/26	48/50	46/48	43/47	43/43	45/38	38/41
Left/right handed	4/43	7/90	11/83	8/82	9/77	7/76	4/75
Education							
University	25	61	63	59	61	45	47
A′ Levels	11	16	12	17	16	18	14
GCSE grade	8	11	13	11	8	14	14
None over 16	3	9	5	3	1	6	4
MMSE	29.2 (1.2)	29.5 (0.9)	29.1 (1.2)	29.3 (1.0)	29.1 (1.1)	28.7 (1.2)	28.2 (1.5)
Cattell	37.6 (4.0)	37.2 (4.3)	35.2 (4.3)	33.7 (4.5)	30.9 (5.6)	27.3 (5.6)	24.3 (5.5)
M-RT	467.5 (58.5)	477.9 (75.8)	537.6 (90.3)	554.4 (85.9)	611.1 (109.1)	669.0 (131.5)	767.3 (166.0)
SD-RT	78.5 (26.2)	78.1 (22.7)	95.1 (30.4)	96.1 (29.3)	122.4 (45.0)	143.4 (57.0)	174.4 (73.7)
Story recall	14.7 (3.8)	15.2 (3.6)	14.1 (3.8)	13.8 (3.7)	12.7 (4.1)	11.1 (4.1)	10.3 (4.1)

Values in parentheses are standard deviations.
Key: Cattell, Cattell culture fair test of fluid intelligence; MMSE, mini mental status examination; M-RT, mean response time on the choice response time task (in milliseconds); SD-RT, intraindividual response time variability on the choice response time task (in milliseconds); story recall, story recall from the Wechsler Memory Scale.

plus 3 images acquired with a b-value of 0. These parameters were optimized for estimation of the diffusion kurtosis tensor and associated scalar metrics. Other DWI parameters were TR = 9100, TE = 104 ms, FOV = 192 mm × 192 mm, voxel size 2 mm × 2 mm × 2 mm, 66 axial slices, and acquisition time 10 minutes and 2 seconds.

2.4. Functional data preprocessing

The data were preprocessed using both analysis of functional neuroimages (AFNI; version AFNI_17.1.01; https://afni.nimh.nih.gov) and the statistical parametric mapping (SPM12) software (http://www.fil.ion.ucl.ac.uk/spm), as called by the automatic analysis (AA) batching system (http://imaging.mrc-cbu.cam.ac.uk/imaging/AA). This was done to combine the advantages of multi-echo independent component analysis (ME-ICA) denoising (AFNI) with DARTEL interparticipant alignment in SPM, which allows for the transformation to an age-representative template that is subsequently transformed to Montreal Neurological Institute (MNI) space. ME-ICA seems to be a very promising method for removal of non-BOLD–like components from the fMRI data, including effects of head motion. It has been shown to improve sensitivity and reduce false positives in both rest (Kundu et al., 2012) and task data (Gonzalez-Castillo et al., 2016). The AFNI parts of the pipeline used the default AFNI preprocessing settings, using the meica.py algorithm (Kundu et al., 2012). This included deobliquing of each TE, slice time correction, and realignment of each TE to the first TE in the run. Then ME-ICA was used to denoise the data for each participant. The details of this procedure are described in (Kundu et al., 2012) and briefly summarized here. For each participant, principal component analysis was used to reduce the dimensionality of the data. This procedure selects all signals resembling correlated phenomena or MR signal for ICA decomposition while excluding thermal noise. Next, FastICA was used to identify spatially independent components, which were characterized as high-kappa, BOLD-like components (signal) and low-kappa, not-BOLD–like components (noise). The ME-ICA–denoised data were reconstructed from the high-kappa components that did not localize to venous structures.

Coregistration and interparticipant alignment of these ME-ICA denoised data were done using the transformations obtained in the previously described AA pipelines that were used to analyze all the Cam-CAN data (see Taylor et al., 2017) and the data of our previous study on the same topic (Campbell et al., 2015). The analyses in the AA pipeline were performed on an optimally combined image, which is the average of the 5 echo times, weighted by their estimated T2* contrast. These optimally combined images were only used to obtain the DARTEL flowfields and MNI transformations. Before the normalization step, the optimally combined images were slice time–corrected, realigned to the first image in the run, and coregistered to the T1 image. The T1 and T2 images were combined to segment various tissue classes, including gray matter (GM), WM, and cerebrospinal fluid (CSF). Next, a sample-specific anatomical template was created for each session, based on the GM and WM segments for each participant, using the DARTEL procedure to optimize interparticipant alignment. The template was then transformed into MNI space, using a 12-parameter affine mapping. Finally, the ME-ICA denoised data were aligned to the optimally combined images, using rigid body alignment. Then the DARTEL flowfields and MNI transformations were applied to the ME-ICA denoised data. The success of this coregistration and normalization procedure was verified by correlating local image intensity values across participants and visually inspecting the data. For 30 participants, there was either a problem with running the ME-ICA denoising or a problem with the normalization; these participants were not included in further analyses. The segmented images were also used to create WM and CSF masks for each participant by selecting only voxels with less than 1% of GM and more than 80% of WM/CSF. After normalization, the data were smoothed with an 8-mm full width at half maximum (FWHM) kernel, and signals were extracted from 748 of the 840 regions defined by Craddock et al. (2012). Only 748 regions were included because they had sufficient coverage in our recent article (Geerligs et al., 2015b), which allowed us to use existing network labels defined in our previous study. To quantify the head motion for each participant, the root mean square volume-to-volume displacement was computed using the approach of Jenkinson et al. (2002). We found that the mean level of head motion was correlated with participant age ($r = 0.5$, $p < 0.001$), and the number of components removed by the ME-ICA denoising was higher for older participants ($r = 0.51$, $p < 0.001$). Participants who had a high level of mean head motion (2 SDs above the mean, 32 participants) and participants for whom nearly all components were removed during the ME-ICA denoising (>88% of all components, 2 participants) were not included in the analyses. Participants excluded in this step tended to be older than the participants who were included (mean age included = 53 years, mean age excluded = 68 years, $t(609) = -4.51$, $p < 0.001$). This left a final sample of 577 participants.

Because of the association between age and head motion, we look extra care to remove head motion confounds from the data. Therefore, in addition to ME-ICA denoising, we reduced any residual effects of motion and other noise confounds on FC results by applying a general linear model (GLM), as it has previously been

shown that ME-ICA denoising can leave some residual motion confounds (Power et al., 2015). This model included expansions of the 6 original motion parameters, as well as of average signals in the WM and CSF from the timecourses of each voxel within each regions of interest (ROI). The WM and CSF signals were created by averaging across voxels in the associated mask image, after normalization but before smoothing. The expansions included the first-order temporal derivative, as well as their squares and squared derivatives, which reduces the effects of motion (Satterthwaite et al., 2013). In total, there were 32 confound and noise regressors. A high-pass filter (0.008 Hz) was implemented by including a discrete cosine transform set in the GLM, ensuring that nuisance regression and filtering were performed simultaneously. To prewhiten the data, the autocorrelation in the GLM error was modeled by a family of 8 exponentials with half-lives from 0.5 to 64 TRs (Geerligs et al., 2017). The autocorrelation hyperparameters were estimated using Restricted Maximum Likelihood Estimation. Efficiency of estimating the autocorrelation hyperparameters was increased by pooling across voxels within each ROI, but done separately for each ROI, to allow for true differences in autocorrelation between functional regions. The autocorrelation model was inverted to prewhiten the data. The whitened residuals of this model were used to estimate the intersubject synchrony and FC.

2.5. Intersubject synchronization

For each participant, we extracted the mean timecourse across all voxels within each ROI. Next, we measured synchronization by correlating each participant's timecourse with a timecourse that was the result of averaging across all other participants. Positive correlation values indicate the presence of a shared signal between 1 participant and all other participants. Correlation values close to zero reflect asynchronous responses across participants. While in analyses of FC, negative correlations or anticorrelations reflect a phenomenon of interest; this is not the case in the current context. Because the synchronization analysis starts with computing a shared signal across participants, anticorrelations cannot be detected. Moreover, it is highly unlikely that there are brain regions with consistent anticorrelations across participants, in which a particular brain region consistently responds in the opposite way in different participants.

The ROI correlation (or synchrony) values were converted to z-scores, using the Fisher r-z transformation, to obtain a more normal distribution. Subsequently, we correlated the synchrony values in each ROI with age. Because of the association between age and head motion, we used the following covariates of no interest in all of our analyses relating intersubject synchronization or connectivity values to other measures: the mean and the maximum of the volume-to-volume displacement values and proportion of independent components removed in the ME-ICA denoising (number of components removed/total number of components). We used regression analyses and Pearson correlations to investigate associations between synchrony, connectivity, age, and other outcome measures. When we identified significant interaction effects (e.g., age by cognition effects), we split the group by age into 3 equally sized subgroups (young, middle, and old) to better understand the nature of the interaction.

Following the analyses relating age to intersubject synchronization, we grouped the ROIs showing a significant age-related decline in synchrony based on the functional brain networks they were in (as identified in Geerligs et al., 2015a,b). In the remainder of the analyses in this article, we focused on those brain networks that had the greatest number of ROIs with significant age-related declines (see results and supplementary results for more details). Three clusters were identified that encompassed ROIs from the FPCN, mPFC, and the MTL. For further analyses, we created average synchrony scores per cluster by averaging across all the ROIs within a cluster.

To determine how intersubject synchronization varied over time, we used a sliding window analysis. We used a tapered-cosine (Tukey) window of width $w = 20$ TRs with a total taper section of length 10 TRs. We slid the windows 1 TR (or time point) at each step. This gave us a measure of intersubject synchronization for each of 177 time windows. To check how the results were affected by the window length, the analyses were repeated for different window lengths (15 and 30 TRs). To be able to relate changes in intersubject synchronization over time, to frames in the movie, we computed a mean intersubject synchronization value for each TR. For each time point, we computed a weighted average of the synchronization values in all the sliding windows that took this time point into account (weights were based on the original cosine window). Then we investigated variations over time in mean intersubject synchronization and in the association between age and intersubject synchronization. Finally, to identify those times in the movie that were particularly affected by age, for each time point, we investigated whether the association between age and synchronization was significantly different from the mean correlation between age and synchronization across all time points. To this end, we phase randomized the intersubject synchronization time series for each participant. This was done by computing a Fourier transform of the time series and replacing the actual phase of the different frequencies by random phases. Different random phases were used for different participants. This way we could compare the actual age effect at each time point to the age effect that would be expected if there were no real differences over time. We indicated time points that were significantly different from the mean age effect after Bonferroni correction for multiple comparisons. To relate the synchronization timecourse to events in the movie, we converted the TRs to seconds (multiply by 2.47) and subtracted 5 seconds from the BOLD timing to account for the delay in the hemodynamic response. We also used the phase randomized data to investigate whether the synchronization timecourses were more similar across the 3 brain clusters than expected by chance. For this analysis, we used the same random phases for different participants, but different random phases for each of the 3 clusters.

2.6. Cognitive measures

Participants performed several cognitive tasks outside the scanner as part of a larger test battery (Shafto et al., 2014). Here, we focus on measures of general cognitive function. Fluid intelligence was measured by the Cattell Culture Fair, a timed pen-and-paper test in which participants perform a series of nonverbal puzzles (Cattell and Cattell, 1960). Verbal memory was measured using delayed recall performance on the logical memory test from the Wechsler Memory Scale Third UK edition, in which participants listen to 2 brief stories and recall them 25–30 minutes later (Wechsler, 1999). Participants also performed a choice response time (CRT) task. In the CRT task, participants used a 4-button response box to respond as quickly as possible to 1 of 4 possible cued fingers (67 trials). There was a variable intertrial interval with a mean of 3.7 seconds. Participants responded correctly to 93.1 % of the trials in CRT. Only these correct trials were used to compute the response time measures. In addition, outlier RTs that were >3 SDs away from an individual's mean were removed (CRT 1.3% of correct trials on average). The mean (M-RT) and the response time variability (SD of RT values, SD-RT) were computed from remaining trials, and inverted ($y = x^{-1}$) to obtain a more Gaussian distribution across participants. Due to this inversion, higher scores are related to better performance for each of the cognitive measures. Because response time variability is strongly related to M-RT, we included M-RT as an additional covariate in analyses relating synchrony to SD-RT (Campbell et al., 2015). Participants with less than 50%

correct on the CRT task were excluded from the analysis; in addition, some participants had missing data for one or more cognitive tests. The final number of participants was 562 for the Cattell test of fluid intelligence, 576 for verbal memory, and 527 for the CRT task.

2.7. Community structure

We investigated whether there were subgroups of participants (or older adults) who consistently responded to the movie in a different way from others, leading to the observed decline in synchronization. To answer this question, we used a weighted stochastic block model (WSBM) to identify participant communities (Aicher et al., 2013). As the input to the algorithm, we computed a mean timecourse for each subject across all ROIs within each of the 3 clusters of brain regions that were defined previously (see Section 2.5) and then computed a correlation matrix representing the similarity between each pair of participants in each cluster. WSBMs are uniquely able to identify relevant types of community structures, because they group connections with similar structural roles in the network. A modular community structure would reveal that evoked responses of participants in one community are more similar to each other than to those of participants in another community. A core-periphery community structure would show a grouping of participants with different levels of synchrony: participants with the most representative or strongest evoked responses form the core, while the other participants represent the periphery. We varied the number of communities (k) from 2 to 8 and for each k, we repeated the community detection 250 times with a random initialization. The WSBM can be driven by both the absence or presence of connections and by the connection weights. The parameter α determines the trade-off between the two. Because we used the unthresholded correlation matrix between participants as the input to the algorithm, we based the community detection only on these weights and not on the absence or presence of certain correlations (fixing the parameter α to 1). The algorithm was implemented in MATLAB using code made available at the author's personal website (http://tuvalu.santafe.edu/~aaronc/wsbm/).

2.8. Functional connectivity

Next, we investigated how individual differences in synchronization were related to differences in FC. FC estimates were obtained for each participant by computing the correlation between the timecourses of each ROI pair. In previous work (Geerligs et al., 2017), we have demonstrated that differences in mean FC between participants can stem from differences related to heart rate variability and that mean regression is an effective way to correct for this. Therefore, we applied mean regression to our FC estimates. For each ROI pair, the mean connectivity was regressed onto the connectivity estimates of that pair and the residuals of that regression were retained for further analysis. This was done using a regression model with an intercept term, which modeled the average connectivity across all participants. The mean connectivity across participants was added back onto the connectivity estimates of each participant after mean connectivity had been regressed out.

To relate connectivity to synchrony, we used Pearson correlations. For each cluster of brain regions, we quantified synchrony as the mean synchrony score across all ROIs within that cluster. Because the synchrony scores in the MTL, FPCN, and mPFC were highly correlated, we looked at connectivity patterns that were uniquely related to the cluster of interest, by partialing out the synchrony scores in the other 2 clusters (in addition to the standard covariates of no interest; the mean and the maximum volume-to-volume displacement values and proportion of components removed in the ME-ICA denoising). The false discovery rate for these correlations was controlled using the Benjamini and Yekutieli (2011) procedure (at $p < 0.05$). We found a large number of ROI pairs where connectivity was related to synchrony. To obtain a summary connectivity score for further analyses, we used a leave-one-out approach. For each participant, we computed the correlation between synchrony and connectivity across all other participants in the sample. We then computed an average connectivity score for the left-out participant for the connections that were significantly ($p_{FDR} < 0.05$) positively related to synchrony in the rest of the group and (separately) for the connections that were negatively related to synchrony in the rest of the group. This gave us two connectivity estimates per participant (similar to Shen et al., 2017). We could then use these connectivity scores to investigate (among other things) if differences in FC mediate age-related differences in intersubject synchrony.

2.9. WM microstructure

To look at how FC differences relate to differences in the WM microstructure, we computed mean kurtosis (MK) from the diffusion data. The diffusion data were optimized for estimation of the MK of the tissue's water diffusion (Shafto et al., 2014). MK is believed to offer a sensitive metric of age-related changes of WM microstructure, such as changes of cell membranes, organelles, and the ratio of intracellular and extracellular water compartments (Falangola et al., 2008).

All preprocessing and modeling of the DWI data was performed using a combination of functions from FSL version 5.0.8, SPM12, and custom scripts written in C and MATLAB, integrated in AA. The DWI data were coregistered to the T1 image, using the average of the 3 $b = 0$ images for each subject, next the data were skull-stripped using the BET utility in FSL. Linear fitting of a higher-order tensor was used to estimate MK. Finally, images of the diffusion metrics were normalized to MNI space using the DARTEL affine transformations from the T1-T2 pipeline described previously. The resulting MK images in MNI space were smoothed with a 1-mm FWHM Gaussian kernel to reduce residual interpolation errors, and the mean MK values in various ROIs was computed (these ROIs are presented below). Traditionally, DWI data are motion corrected at the postacquisition level by using image registration techniques to coregister each DWI to the first acquired $b = 0$ image. However, this technique will fail to correct for distortions and motion when high b-values are used and may introduce other artifacts (Ben-Amitay et al., 2012). For this reason, we did not apply registration-based motion correction to the DWI data in this study. Detection and exclusion of outliers were performed at the analysis level to avoid including data sets affected by other artifacts and distortions. Participants with severe head motion during the DWI scan, as revealed by striping in the diffusion data (Neto Henriques and Correia, 2015), were excluded and participants with MK values in a given ROI of 3 SDs above or below the group average were also excluded. The final sample varied between 498 and 505 participants in each of the ROIs.

The ROIs that we used to compute the mean MK values were defined by the Johns Hopkins University WM tractography atlas (Hua et al., 2008). These included the uncinate fasciculus, superior longitudinal fasciculus, inferior fronto-occipital fasciculus, anterior thalamic radiations, forceps minor, forceps major, cerebrospinal tract, the inferior longitudinal fasciculus (ILF), ventral cingulate gyrus (CINGHipp), and the dorsal cingulate gyrus (CING). Total intracranial volume was used as a covariate in all analyses that included MK measures.

3. Results

Participants in the study watched a shortened version of a movie by Alfred Hitchcock, "Bang! You're Dead" (Shafto et al., 2014). This

movie is about a young boy who mistakes his uncle's revolver for a toy gun. He plays with the partially loaded revolver at home and in public, resulting in a number of moments where it appears as if he might shoot someone. The movie elicited synchronized brain activity over participants in all of the 748 ROIs that were distributed across the whole brain. The strongest synchronization was found over the visual and auditory cortices, while subcortical and more frontal regions of the brain were less synchronized (see Fig. 1A). In line with our previous work (Campbell et al., 2015), we observed that the synchronization between each participant and the mean timecourse of the group declined with age (Fig. 1B). Age-related reductions in synchronization were most apparent over left and right inferior parietal regions, the right middle frontal gyrus, and the medial prefrontal gyrus. We also observed significant differences in the hippocampus and parahippocampal areas (bilateral), the left and right caudate and the thalamus, bilateral postcentral and supramarginal gyri, the insula (bilaterally), lingual gyrus, the cingulum, and dorsal parts of the cerebellum. We did not observe any significant positive correlations between age and synchrony. Additional analyses suggest that these effects of age cannot be explained by age-related changes in the amount of noise in the data or by the amplitude of evoked responses (see supplementary results and Fig. S1); therefore, they most likely reflect an age-related increase in the idiosyncrasy of neural responses to the events in the movie.

Interestingly, synchrony appears to be preserved with age in a number of regions (Fig. 1B). To test the evidence in favor of this apparent lack of difference, we computed Bayes factors by comparing regression models with and without effects of age on synchrony (Wetzels and Wagenmakers, 2012). Bayes factors were grouped into categories (Jeffreys, 1961) to give an indication of the strength of the evidence for preserved synchrony with age or for a decline in synchrony with age (see Fig. 1C). Regions that showed strong evidence for preservation of synchrony with age included the language network bilaterally (inferior frontal gyrus [IFG], particularly on the left, and bilateral middle temporal gyrus), the right TPJ, dorsal parts of the precuneus, the supplementary motor area, left and right precentral gyrus, and the left and right putamen. Regions with decisive evidence for age-related synchrony decline largely overlapped with the areas showing significant age-related

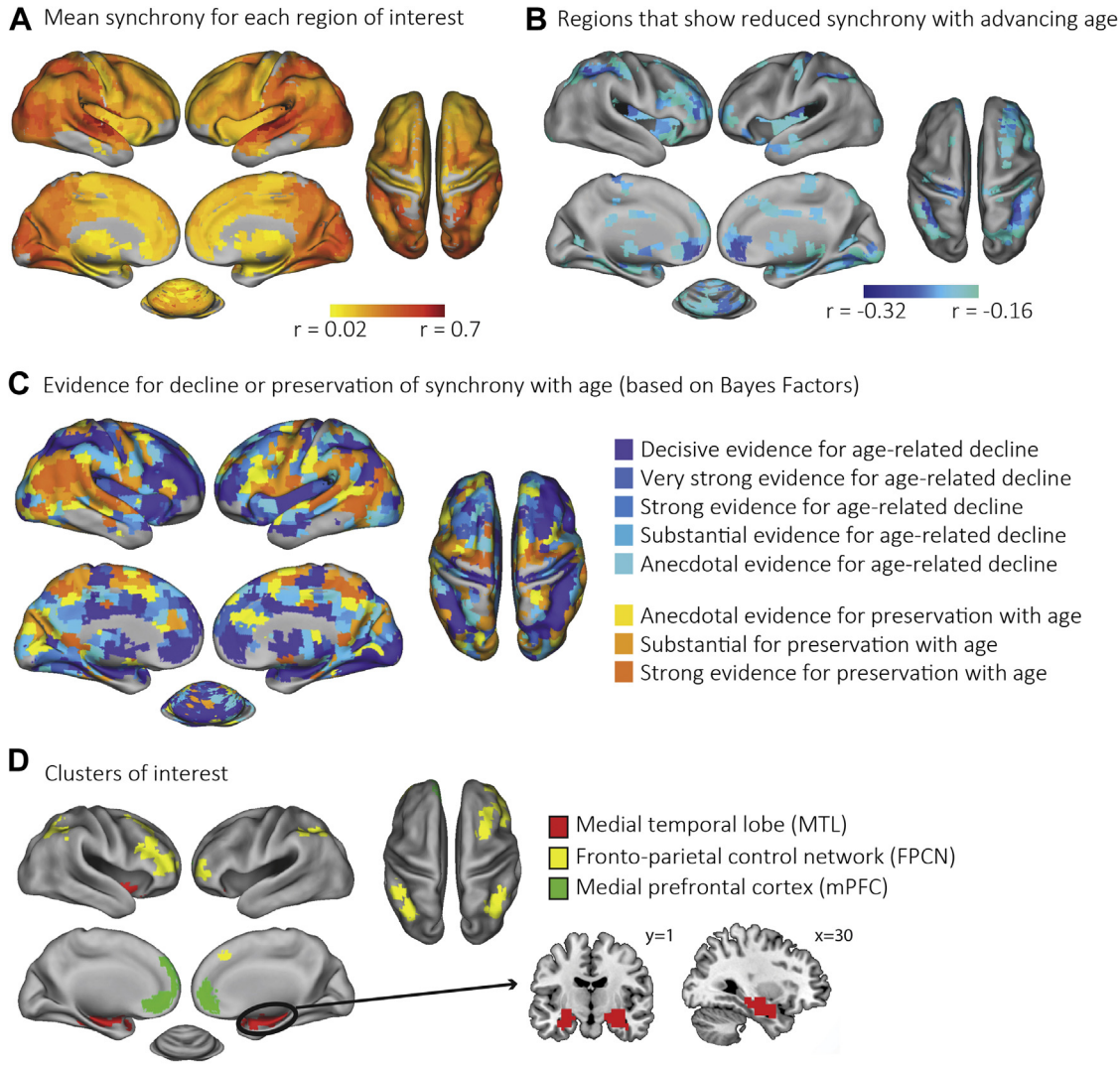

Fig. 1. (A) Significant intersubject correlations were seen in all cortical and subcortical regions of interest. (B) Synchronization was negatively correlated with age in several regions. Analyses in A and B were Bonferroni corrected for multiple comparisons. (C) Evidence for decline or preservation of synchrony based on Bayes factors. Regions were colored based on the Bayes factor categories (Jeffreys, 1961). One region (not visible on the surface projection) showed anecdotal evidence for an age-related increase in synchrony. (D) The clusters that were used in further analyses. Results in A–C were adjusted for covariates of no interest related to head motion and ME-ICA denoising. Abbreviations: ME-ICA, multiecho–independent component analysis.

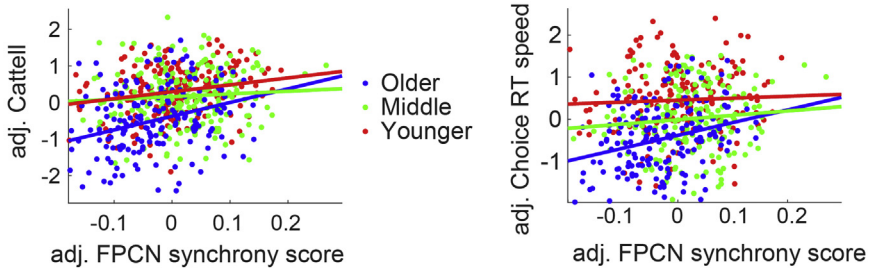

Fig. 2. Scatter plot for the association between performance on the Cattell test and response speed in the choice RT task and synchrony in the FPCN. The scores were adjusted for the covariates of no interest related to head motion and ME-ICA denoising. Abbreviations: FPCN, frontoparietal control network; ME-ICA, multiecho independent component analysis.

decline in Fig. 1B (these were described previously). Other areas that showed very strong/strong evidence for age-related decline included the lingual gyrus and ventral parts of the precuneus.

In the remainder of the article, we explore the nature and potential causes of the observed age-related asynchrony within those networks (or parts of networks) (see Fig. 1D) that contained the greatest number of ROIs with significant age-related declines (for details of the selection approach see supplementary results and Fig. S2). We focus on clusters in the FPCN, mPFC, and the MTL, as these areas not only showed the strongest age-related declines (indicated by darker blue in Fig. 1B) but are also repeatedly implicated in the neurocognitive aging literature (Turner and Spreng, 2015). While the FPCN is critical for cognitive control and working memory (Vincent et al., 2008), areas in the MTL are associated with memory encoding and retrieval (Moscovitch et al., 2016) and the mPFC is associated with memory, imagination, and affective processing (Benoit et al., 2014; Van Kesteren et al., 2012; Winecoff et al., 2013). For each cluster, average synchrony scores were computed by averaging synchrony scores across ROIs. After this averaging step, the association between age and synchrony was $r(575) = -0.31$ ($p < 0.001$) for the FPCN, $r(575) = -0.32$ ($p < 0.001$) for mPFC, and $r(575) = -0.33$ ($p < 0.001$) for MTL. Synchrony scores were strongly correlated across these 3 networks [FPCN-mPFC, $r(575) = 0.73$, $p < 0.001$; FPCN-MTL, $r(575) = 0.66$, $p < 0.001$; mPFC-MTL, $r(575) = 0.71$, $p < 0.001$]. In the following sections, we aim to determine the cause of age-related declines in these clusters.

3.1. Sensory loss

The first potential cause we examined was whether reductions in intersubject synchrony could be due to a problem with perceiving the stimuli. If this was true, we would expect the most substantial effects of age in visual and auditory cortices and we would expect no effect of age in higher-order regions after accounting for effects in primary sensory regions. However, we observed that the age-effects on synchrony were not stronger in the primary visual and auditory regions than in other networks. We did observe strong or decisive evidence for age-related decline in the lingual gyrus and fusiform gyrus, extending into the calcarine sulcus as well as some ROIs in the middle occipital gyrus, primarily in the right hemisphere. However, many ROIs in the cuneus, extending into the calcarine and the superior occipital gyrus show anecdotal or weak evidence for preservation, not decline with age. Most ROIs in medial regions in the auditory network, including Heschl's gyrus, showed either decisive or very strong evidence for age-related decline. However, more lateral regions tended to show only weak evidence for decline (Fig. 1C).

We also tested whether age differences in synchrony in visual and auditory regions could explain age-related synchrony differences in the mPFC, MTL, and FPCN. To this end, we constructed 2 summary scores, 1 for the visual and 1 for the auditory network, which contained the mean synchrony across all ROIs that showed a (Bonferroni-corrected) significant effect of age on synchrony (19 visual and 11 auditory; see Fig. 1B). We observed that age-related synchrony differences in the mPFC, MTL, and FPCN were highly

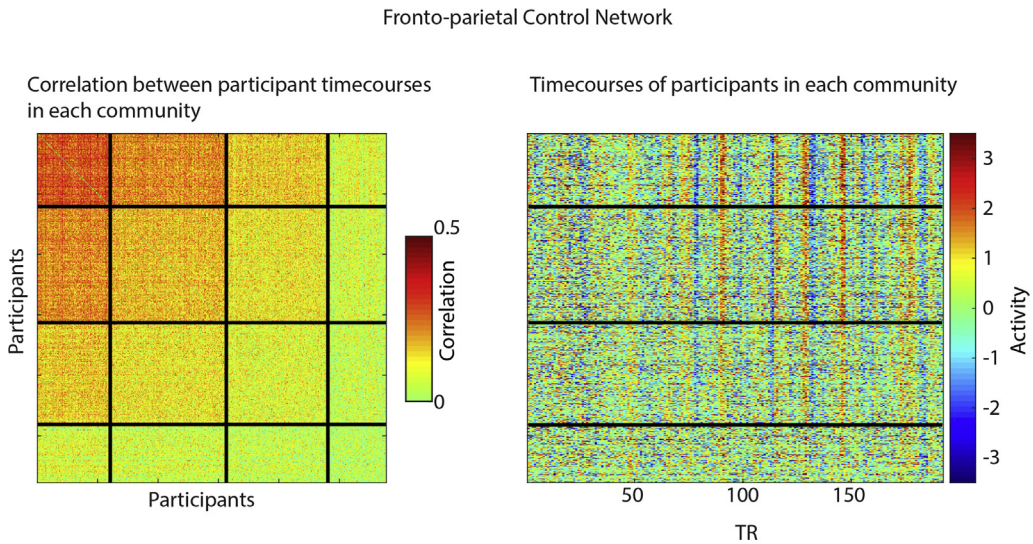

Fig. 3. Community structure for k = 4, for the FPCN. The figure on the left shows the correlations between the timecourses of all participants, both within and between the different communities. Communities are ordered from the highest to the lowest intersubject synchrony. The figure on the right shows the FPCN timecourse for each participant in each of the communities. This figure demonstrates that less synchronous individuals did not simply show a lower amplitude of responding. Abbreviation: FPCN, frontoparietal control network.

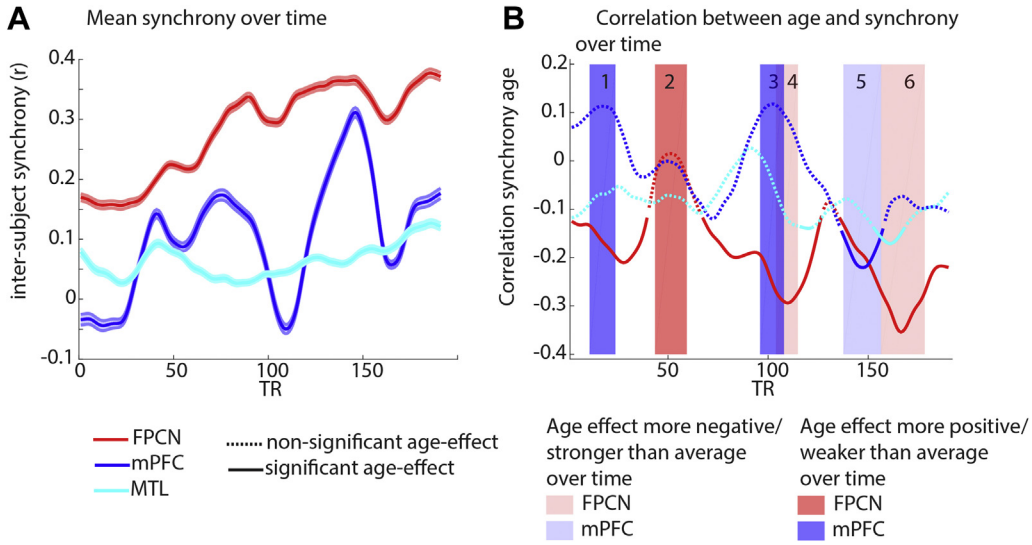

Fig. 4. Changes over time in intersubject synchrony for (A) the mean across the group and (B) the effect of age on intersubject synchrony. In panel A, the mean is represented by the line and the standard error around the mean is shown by the shaded regions around the lines. In panel B, time points where the age-effects were significantly stronger or weaker than average are shown in light (stronger than average) or dark (weaker than average) patches (after a nonparametric equivalent of Bonferroni correction accounting for dependencies between time points). Numbers correspond to moments in the film discussed in the text. Dotted lines indicate associations between age and synchrony that did not reach significance while continuous lines indicate significant associations (after an FDR correction across all time points). Abbreviations: FPCN, frontoparietal control network; mPFC, medial prefrontal cortex; MTL, medial temporal lobe.

significant even when we covaried out these 2 auditory and visual synchrony summary scores [mPFC, r (575) = −0.20, $p < 0.001$; FPCN, r (575) = −0.16, $p < 0.001$; MTL, r (575) = −0.20, $p < 0.001$]. Effects of age on synchrony even remained significant when we used the synchrony scores of each of the 30 visual and auditory ROIs with significant age-effects as separate covariates of no interest [mPFC, r (575) = −0.18, $p < 0.001$; FPCN, r (575) = −0.13, $p = 0.002$; MTL, r (575) = −0.20, $p < 0.001$]. These results suggest that the effects in these clusters cannot be explained by the input not being perceived by older adults.

3.2. Cognitive functioning

Second, we investigated whether age-related differences in cognitive functioning could explain some of the age-related differences in synchrony. To this end, we investigated the association between intersubject synchrony and the scores on various cognitive tests performed outside the scanner: the Cattell test of fluid intelligence, the logical memory test, and M-RT and RT variability (SD-RT) on the choice RT tasks. We found that there was a significant (Bonferroni-corrected) age by performance interaction explaining FPCN synchrony for the Cattell test of fluid intelligence and for M-RT (Fig. 2 and Table 2). In older adults, there was a strong positive association between synchrony and Cattell [r (177) = 0.30, $p < 0.001$], which was weaker for younger adults [r (181) = 0.21, $p = 0.004$] and absent in the middle-aged group [r (198) = 0.07, $p = 0.31$]. Similarly, for M-RT, we observed a positive association between response speed and synchrony for older adults [r (174) = 0.28, $p < 0.001$], but no significant associations for younger [r (172) = 0.045, $p = 0.56$] or middle-aged participants [r (175) = 0.10, $p = 0.31$] (Fig. 2).

For the mPFC, a similar association between synchrony and M-RT was observed, which was significant in the older [r (174) = 0.32, $p < 0.001$] but not the middle aged [r (175) = 0.10, $p = 0.20$] or the younger groups [r (172) = 0.045, $p = 0.56$]. A similar trend in the MTL did not reach significance (see Table 2).

Because synchrony scores in the MTL, FPCN, and mPFC were highly correlated, we investigated whether these associations remained significant after covarying out synchrony scores in the remaining 2 regions. We found that the effects of Cattell and M-RT on FPCN synchrony remained significant [t (553) = 3.33, $p < 0.001$ and t (518) = 3.41, $p < 0.001$, respectively], but this was not the case for the effect of M-RT on mPFC synchrony [t (518) = 1.94, $p = 0.053$]. These results suggest that reduced synchrony with age within the cognitive control network (FPCN) may be due to concomitant declines in fluid intelligence and processing speed.

3.3. Increased idiosyncrasy with age or subgroups of similar responders?

Next, we investigated if there were subgroups of participants (or older adults) who consistently respond to the movie in a different way, which caused the observed decline in synchronization. This was done by applying a WSBM to identify groups of participants, which we will refer to as “communities.” A modular community structure would demonstrate that evoked responses of participants in one community are more similar to each other than to those of participants in other communities, revealing that there are subgroups of participants who respond to the movie in a different way. Alternatively, the WSBM could identify a core-periphery community structure, in which participants with different levels of synchrony are grouped together. Participants with the most representative or strongest evoked responses form the core of the community of participants, while the other participants represent the periphery. This analysis revealed a core-periphery community structure for each cluster (mPFC, FPCN, and MTL), in that cross-subject correlations were strongest for a core group of subjects and then gradually decreased across participants in more peripheral communities. An example of a community structure of the FPCN with 4 communities is shown in Fig. 3 and the similar results were observed for the mPFC and the MTL and varying numbers of communities (2–8, see Fig. S3). Thus, no evidence was observed for modular communities, suggesting that there are not subgroups of participants (of any age) who are consistently responding to the movie in a different way.

In line with our observation of a reduction in synchrony with advancing age, we observed that participants in less synchronous

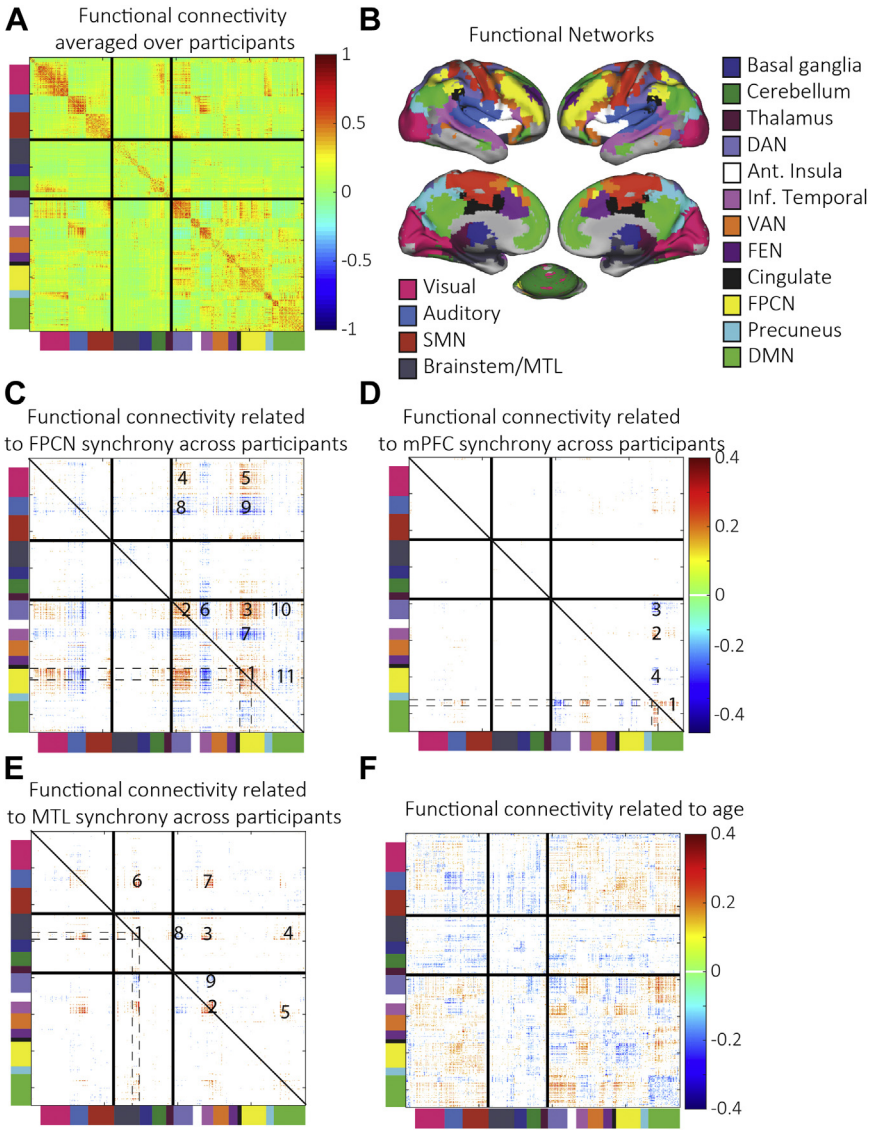

Fig. 5. (A) FC averaged across participants. (B) Functional networks definitions that were used (Geerligs et al., 2015b). (C–E) Significant correlations between intersubject synchrony and connectivity across participants, adjusting for effects of age, for the FPCN, mPFC, and MTL clusters, respectively. (F) Significant correlations between age and FC. Results in (C–F) were corrected for multiple comparisons using a false discovery rate (FDR) correction (Benjamini and Yekutieli, 2011). Numbers in the top right half of the matrices (C–E) correspond to findings of interest discussed in the text. As each figure is symmetrical, the same findings can be observed without numbers on the left bottom side of the figure. Dotted lines indicate the ROIs included in each cluster and their connections to the rest of the brain. Solid lines indicate the borders between sensorimotor networks (top) subcortical networks (middle) and higher-order cortical networks (bottom). Abbreviations: Ant, anterior; DAN, dorsal attention network; DMN, default mode network; FC, functional connectivity; FEN, fronto-executive network; FPCN, fronto-parietal control network; Inf., inferior; MTL, medial temporal lobe; MPFC, medial prefrontal cortex; ROIs, regions of interest; SMN, somatomotor network; VAN, ventral attention network.

communities tended to have a higher age. This was true for the each of the 3 cluster and across all numbers of communities (2–8). Here we show the results for 4 communities, where the mean age increased from the most-to-least synchronized communities in the FPCN (44 years, 48 years, 56 years, 68 years), the mPFC (44, 48, 56, and 68 years), and the MTL (42, 47, 58 and 67 years). An ANOVA revealed that these age differences between communities were highly significant in all 3 clusters [FPCN; $F(3573) = 46.62$, $p < 0.001$; mPFC $F(3573) = 50.23$, $p < 0.001$; MTL $F(3573) = 52.14$, $p < 0.001$].

The right panel of Fig. 3 shows the timecourses of participants in different communities. This figure illustrates that the reduction in synchrony is driven by positive and negative evoked responses to events in the movie, which are shared between participants in the highly synchronous communities, but less so between participants in the low synchronized communities. In the supplementary results and Supplementary Fig. S1, we also show that differences between participants cannot be fully explained by differences in the amplitude of the evoked responses. Together, these results suggest that differences in synchrony with advancing age are at least partly driven by the more idiosyncratic nature of the evoked responses in older adults (Fig. 3).

3.4. Time-dependent changes in synchrony

The previous analyses revealed that participants' responses to the movie become more idiosyncratic with age. However, it is not clear if there are specific moments in the movie that cause this reduction in synchronization. To answer this question, we used sliding window correlations to investigate the intersubject synchrony in different sections of the movie.

Table 2
Associations between synchrony scores and performance on 4 cognitive tests

A. FPCN synchrony					
Model component	Statistic	Cattell	M-RT	SD-RT	Story recall
Full model	R2	0.44	0.47	0.47	0.44
	F	73.45[a]	75.65[a]	56.71[a]	73.26[a]
	p-value	<0.001	<0.001	<0.001	<0.001
Effect of performance	T	2.57	0.66	0.84	2.44
	p-value	0.011	0.508	0.400	0.015
Interaction between age and performance	T	3.58[a]	5.45[a]	−0.06	1.72
	p-value	<0.001	<0.001	0.955	0.085
B. mPFC synchrony					
Model component	Statistic	Cattell	M-RT	SD-RT	Story recall
Full model	R2	0.44	0.46	0.46	0.44
	F	72.52[a]	75.25[a]	56.22[a]	75.48[a]
	p-value	<0.001	<0.001	<0.001	<0.001
Effect of performance	T	1.61	0.75	0.09	1.41
	p-value	0.107	0.454	0.931	0.160
Interaction between age and performance	T	1.43	4.66[a]	0.01	−0.16
	p-value	0.153	<0.001	0.995	0.873
C. MTL synchrony					
Model component	Statistic	Cattell	M-RT	SD-RT	Story recall
Full model	R2	0.46	0.49	0.49	0.47
	F	80.24[a]	82.44[a]	61.68[a]	84.11[a]
	p-value	<0.001	<0.001	<0.001	<0.001
Effect of performance	T	0.76	−0.50	−0.29	1.33
	p-value	0.449	0.619	0.770	0.185
Interaction between age and performance	T	0.80	3.06	0.41	−1.39
	p-value	0.424	0.002	0.683	0.164

In each regression model, synchrony scores were predicted by age, performance on one of the 4 cognitive tests, the interaction between age and performance, and the covariates of no interest related to head motion and ME-ICA denoising. For SD-RT, M-RT was included as an additional regressor of no interest. The final number of participants was 562 for the Cattell test of fluid intelligence, 576 for story recall, and 527 for the choice response time task.
Key: FPCN, frontoparietal control network; mPFC, medial prefrontal cortex; MTL, medial temporal lobe; ME-ICA, multiecho–independent component analysis; M-RT, mean response time on the choice response time task (in milliseconds); SD-RT, intraindividual response time variability on the choice response time task (in milliseconds).
[a] Significant after Bonferroni correction for multiple comparisons.

Mean synchrony increased over time in both the mPFC and the FPCN and changes in synchrony were significantly positively correlated between these 2 clusters ($p = 0.005$, Fig. 4A). Although both clusters showed an increase in synchrony over time as the storyline built up, mPFC synchrony showed large fluctuations in synchrony over time, while FPCN synchrony showed a more gradual increase. In the MTL, we observed lower levels of synchrony overall and a gradual increase in synchrony as the movie progressed. Synchrony changes in the MTL were not significantly related to synchrony changes in the mPFC ($p = 0.13$) or the FPCN ($p = 0.34$).

We investigated the change over time in the association between age and synchrony in each of the networks. Because the sliding window analysis relies on fewer time points to compute the synchrony measures, the associations between age and synchrony were generally weaker than those when the whole time series is used to compute synchrony. For each of these networks, we already knew that older age was associated with reduced synchrony. In this analysis, we wanted to investigate whether there were time points that deviated significantly from this mean trend. This way, we could identify if there was significant variation between time points in the associations between age and synchrony. Therefore, we identified moments in the movie when the association between age and synchrony was particularly weak or pronounced in each cluster (see Methods), compared to the average effect of age over time. For the MTL, no significant differences from the mean were observed over time after Bonferroni correction. However, for the mPFC and FPCN, we found moments with relatively weak or strong associations between age and synchrony (Fig. 4B). These moments are numbered in Fig. 4B, and the same numbering is used in the descriptions in the remainer of this section. Results were highly similar when a different size of sliding window was used in the analysis (see Fig. S4 and Fig. 4).

For the mPFC, age differences were minimal (or even positive) at points in the movie when there was low mPFC synchronization across all participants (see Fig. 4A). The first of these moments (1 in Fig. 4B, around TR = 10–23) is at the start of the movie; the boy is playing with his friend, then enters the house, and listens to a conversation. The other is when the boy is listening to a conversation between his parents and uncle, just before he leaves the house and walks through town (TR = 96–108; moment 3). At these moments, there were no particularly salient events in the movie and therefore there may have been low synchronization in both older and younger adults.

The time point with the strongest age-related decline in mPFC synchrony is during a scene (TR = 138–157; moment 5) where the boy puts extra bullets in the revolver and it seems like he might shoot a man. This is also a moment where there is particularly strong mPFC synchrony across all participants, suggesting that information processing in the mPFC is similar across participants at this point in the movie; however, less so for older than younger participants.

Age differences in the FPCN were minimal at the critical moment when the boy finds his uncle's revolver and loads it with bullets (TR = 43–59; moment 2). Around this same time, synchrony peaks in the mPFC and MTL (see Fig. 4A around TR = 40) and the FPCN (around TR = 48).

The first moment in the movie when there is a particularly negative association between age and FPCN synchrony (TR = 104–115; moment 4) overlaps with a moment when mPFC synchrony is positively associated with age (TR = 96–108; moment 3). This is during a slow scene where the boy is walking through town. The other moment when age-effects on FPCN synchrony were

especially pronounced was during the lengthy scene (around TR = 157–179; moment 6) in which the boy interacts with a man and his daughter. Interestingly, these 2 moments with low levels of suspense introduced the largest age-related changes in FPCN synchrony.

Our findings demonstrate that although synchrony differences in mPFC and FPCN are highly correlated, they do appear to originate from separable processes, as the age-related differences in synchrony occur at different times in these 2 clusters.

3.5. Relation between FC and synchrony

To examine the role of the 3 clusters during movie watching in their broader network architecture, we investigated the association between FC and synchrony. Fig. 5A shows the FC between all ROIs, averaged across participants. In a previous article, we demonstrated that this connectivity pattern is very similar to the typical resting state FC (Geerligs et al., 2015b). Because we were interested in a direct association between synchrony and connectivity, we looked at these associations over and above effects of age. Furthermore, because the synchrony scores in the MTL, FPCN, and mPFC were highly correlated, we looked at connectivity patterns that were uniquely related to the cluster of interest by partialing out the synchrony scores in the other 2 clusters.

For the FPCN (Fig. 5C), we found that higher synchrony was associated with stronger connectivity within the FPCN (see element 1 in Fig. 5C), within the dorsal attention network (DAN, element 2) and between the DAN and the FPCN (element 3), as well as between the visual networks and the DAN (element 4) and the FPCN (element 5). In addition, higher synchrony was related to lower connectivity (or more negative connectivity) between the inferior temporal network and the DAN (element 6) and FPCN (element 7), between the auditory network and the DAN (element 8) and FPCN (element 9), and between the default mode network (DMN) and the DAN (element 10) and FPCN (element 11).

Synchrony in the mPFC (Fig. 5D) was associated with connectivity between the mPFC and the rest of the DMN (see Fig. 5D, element 1) as well as between the mPFC and the inferior temporal network (element 2). It was also associated with lower (or more negative connectivity) between the mPFC and the DAN (element 3) and between the mPFC and the FPCN (element 4).

For the MTL (Fig. 5E), we found that higher synchrony was associated with stronger connectivity within the MTL (see Fig. 5E, element 1) and the inferior temporal network (element 2). Connectivity between these 2 networks was also increased with higher synchrony (element 3). In addition, connectivity between the MTL and the DMN (element 4) and between the DMN and the inferior temporal network (element 5) was higher with higher synchrony. The auditory network also showed stronger connectivity to both the MTL (element 6) and the inferior temporal network (element 7). Higher MTL synchrony was associated with lower connectivity (or more negative connectivity) between the DAN and the MTL (element 8), as well as between the DAN and the inferior temporal network (element 9). These findings support the results from the sliding-window analysis in demonstrating that although synchrony differences in MTL, mPFC, and fronto-parietal network are highly correlated, they do appear to originate from separable processes (Fig. 5).

To investigate whether these associations between synchrony and connectivity may mediate some of the age-related differences in synchrony, we also examined the association between age and connectivity. In line with previous studies (Chan et al., 2014; Geerligs et al., 2015a), we observed that with age, there was a decrease in within-network connectivity and an increase in connectivity between distinct functional networks (Fig. 5B, also see supplementary results). To test for a mediation effect, we constructed an FC summary score for each participant using a leave-one-out approach (see Methods), resulting in a positive and a negative connectivity score for each cluster and each participant. We can interpret these connectivity scores roughly as an average of the negative correlations (negative connectivity scores) and an average of positive correlations (positive connectivity scores) that relate to synchrony in the FPCN, MTL, and mPFC (Fig. 5C–E). We found that for each cluster and for each connectivity score (positive and negative), connectivity differences significantly mediated the association between age and synchrony ($p < 0.001$). These differences explained between 39% and 71% of the association between age and synchrony (see Table 3). However, in each case, the residual association between age and synchrony remained significant even after accounting for the mediating effect of connectivity.

3.6. Relation to WM

In the previous section, we found that the effects of age on synchrony were strongly related to differences in FC. Therefore, we next investigated how these FC differences relate to structural connectivity. In particular, we investigated whether the average FC profiles that related to synchrony (dependent variable) were significantly associated with WM integrity, as measured by MK (independent variable). We used Bonferroni correction to account for multiple comparisons across tracts and connectivity scores, as well as the number of effects of interest. Here, we looked at both main effects of MK and interactions between MK and age because we expected higher variability in WM integrity with advancing age.

We observed a significant interaction [$t(493) = 3.80$, $p < 0.001$] between age and MK in the right ILF for the positive MTL connectivity scores (Fig. 6). To further explore the nature of this interaction, we examined the effect within each age subgroup (young, middle, and old). We found that MK was not significantly related to connectivity in the young group [$r(159) = -0.12$, $p = 0.14$] and negatively related to MK in the middle-aged group [$r(175) = -0.18$, $p = 0.018$]; however, in the older group, we observed a strong

Table 3
Mediation models testing whether changes in connectivity (M) can explain the association between age (X) and synchrony (Y)

Synchrony	Connectivity	a	b	c'	c	ab	%	T-value
FPCN	FPCN-positive FC	−0.28[a]	0.58[a]	−0.15[a]	−0.32[a]	−0.16[a]	51	−5.89
FPCN	FPCN-negative FC	0.33[a]	−0.68[a]	−0.09[b]	−0.32[a]	−0.22[a]	71	−7.64
mPFC	mPFC-positive FC	−0.29[a]	0.43[a]	−0.20[a]	−0.33[a]	−0.13[a]	39	−5.69
mPFC	mPFC-negative FC	0.30[a]	−0.47[a]	−0.18[a]	−0.33[a]	−0.14[a]	43	−6.16
MTL	MTL-positive FC	−0.30[a]	0.59[a]	−0.15[a]	−0.33[a]	−0.18[a]	55	−6.93
MTL	MTL-negative FC	0.29[a]	−0.46[a]	−0.20[a]	−0.33[a]	−0.13[a]	40	−5.99

Path a is between age and connectivity; path b is between connectivity and synchrony; path c is between age and synchrony, without connectivity as a mediator in the same model; path c' is between age and synchrony, with connectivity as a mediator in the same model; path ab is the indirect effect of age on synchrony via connectivity; the % mediation is the relative change of c' compared to c. The right column shows the t-value for the mediation effect (all corresponding p-values were below $p = 0.001$).
Key: FC, functional connectivity; FPCN, frontoparietal control network; mPFC, medial prefrontal cortex; MTL, medial temporal lobe.
[a] $p < 0.001$.
[b] $p < 0.005$.

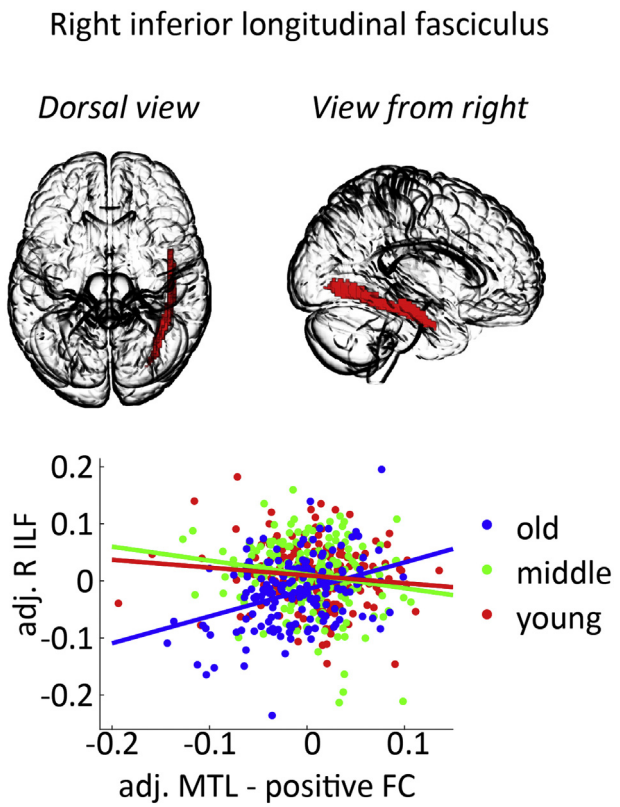

Fig. 6. A significant interaction between age and MK in the right ILF was observed for the positive MTL FC scores. The MK and FC scores were adjusted for the covariates of no interest related to head motion and ME-ICA denoising as well as total intracranial volume. Abbreviations: FC, functional connectivity; ILF, inferior longitudinal fasciculus; ME-ICA, multiecho–independent component analysis; MTL, medial temporal lobe; MK, mean kurtosis.

positive correlation between MK and MTL-related connectivity scores [r (161) = 0.35, $p < 0.001$]. This correlation between MK in the right ILF and MTL-related connectivity scores in the older group is also significant when a Spearman rank correlations is used [r (161) = 0.29, $p = 0.002$], suggesting that the outliers visible in Fig. 6 are not the cause of the observed effect.

4. Discussion

Our results demonstrate that neural processing of naturalistic stimuli is altered with advancing age. Age differences in intersubject synchrony were most pronounced in the FPCN, MTL, and mPFC, while other areas, such as the language network, showed preserved synchrony across the lifespan. Particularly for the FPCN, lower synchrony was related to declines in cognitive functioning on lab-based tasks. Furthermore, it appears that older adults' response to the movie was indeed becoming more idiosyncratic rather than more similar to age-matched peers. We were able to identify distinct temporal profiles and FC patterns that contributed to synchrony declines in different brain regions. These results suggest that there are multiple, separable mechanisms that contribute to the observed age-related declines in synchrony and that declines in different regions were at least partly driven by the content of the movie.

In line with previous studies, we observed evidence for a decline in synchronization with advancing age (Campbell et al., 2015; Oren et al., 2017); however, we were also able to identify a number of regions with preserved synchrony across the lifespan. These included the middle temporal gyri (MTG) and (predominantly left) IFG, dorsal precuneus, and right TPJ. The right TPJ has been associated with reorienting of attention to unattended external stimuli, social cognition tasks, such as perspective taking or empathy and theory of mind (Krall et al., 2015), while the dorsal precuneus has been associated with visuospatial information processing, spatial navigation, and imagery (Zhang et al., 2012). The MTG and the left IFG are part of a functional network involved in language processing (Tyler et al., 2010). It is worth noting that the preserved MTG and left IFG regions identified in the current analysis differ from (and are more extensive than) the MTG and left IFG ROIs that declined with age in Campbell et al. (2015; see their Fig. 6B). Preservation of this language network during naturalistic viewing across the lifespan is in line with previous studies that have emphasized the resilience of this network to the effects of age, particularly during task-free language comprehension (Campbell et al., 2016; Davis et al., 2014). The similarity of information processing in this network across the lifespan suggests that even within the context of a multimodal stimulus, language comprehension appears to be preserved with age.

Most brain regions that showed a significant age-related decline were part of the FPCN, mPFC, and MTL. This is in line with previous research suggesting that these brain regions are particularly age-sensitive, both in terms of functional and structural declines (Geerligs et al., 2015a; Good et al., 2001; Turner and Spreng, 2015). In each of these brain regions, we found that synchrony increased as the movie progressed, in line with the view that these regions are responsible for the creation and maintenance of event models—or representations of the wider plot and story arc (Hasson et al., 2008; Zacks et al., 2010)—that would accumulate over time as the movie progresses. This is also supported by a more in depth exploration of the events in the movie that occur at moments of high synchronization. For example, the first peak in synchronization of all 3 clusters co-occurs with the moment where the main storyline of the movie is revealed (i.e., when the boy finds the uncle's revolver).

Although FPCN, MTL, and mPFC all seem to be involved in representations of the story arc, our results also point to separate roles of these areas in the processing of the information in the movie. The FPCN has previously been associated with cognitive and attentional control (Shulman and Corbetta, 2012; Vincent et al., 2008). Age-related declines in FPCN synchrony were maximal at moments with low levels of suspense and minimal during very engaging scenes. This could indicate that older adults are more prone than young adults to lapses in attentional or cognitive control during slow moments when there is less external capture. This is also in line with the positive association we observed between FPCN synchrony and performance on the Cattell test of fluid intelligence in older participants. Performance on the Cattell test has been associated with a range of cognitive functions including attentional control and working memory (Friedman and Miyake, 2004). On top of that, the FC analyses demonstrated that increased connectivity within and between the FPCN and the DAN, involved in top-down attentional control and eye-movement control (Shulman and Corbetta, 2012), was strongly associated with intersubject synchrony. Together, these results suggest that age-related synchrony declines in the FPCN reflect age-related deficits in attentional or cognitive control during less engaging parts of the movie.

The mPFC has previously been associated with affective processing/integration of incoming information with existing knowledge (Benoit et al., 2014; Van Kesteren et al., 2012). For the mPFC, we found large fluctuations in intersubject synchronization over time. At moments when it was not clear how the movie would progress, there was low intersubject synchronization, while at crucial, revealing moments in the movie (such as when the boy exchanges his toy gun for the uncle's revolver or when it seems the boy might shoot someone), there were sharp increases in intersubject synchronization. This is in line with the proposed roles of

the mPFC in affective processing and simulation of future scenarios based on integration of incoming information with existing knowledge; previous studies have found higher synchrony in this region when participants can integrate incoming information with existing knowledge or schemas (Oren et al., 2017; van Kesteren et al., 2010). Age affected information processing in the mPFC most during salient events, at times when younger adults' responses were highly synchronized; this age-effect may be due to older adults' more individualistic knowledge about the world (Freund and Baltes, 1998; Ramscar et al., 2017) or altered emotional processing (Mather and Carstensen, 2005).

The third cluster of age-related synchrony decline we investigated was in the MTL, a region critical to episodic memory encoding and retrieval (Moscovitch et al., 2016; Preston and Eichenbaum, 2013). In the MTL, we did not observe significant variability in the effect of age on intersubject synchronization over time. However, we did observe an increase in MTL synchrony across participants at the moment the boy exchanges his toy gun for his uncle's revolver. This may reflect the importance of that moment in the narrative sequence, which is similarly encoded by all participants. This is line with previous work showing that there is an increase in hippocampal activity just after an event boundary (Baldassano et al., 2017; Ben-Yakov et al., 2013). Furthermore, the observed age-related decline in MTL synchrony fits well with recent behavioral work showing that older adults are less consistent with others when indicating event boundaries in an ongoing film narrative (Kurby and Zacks, 2011; Zacks et al., 2006), and this increased idiosyncrasy is related to GM volume in the MTL (Bailey et al., 2013). In this study, MTL synchrony was associated with FC within and between the MTL, the MTG, the DMN, and the auditory cortex. This suggests that the auditory content of the movie (including speech) was an important driver of MTL synchrony. In older adults, loss of FC between these regions was associated with a decline in WM microstructure in the right ILF, a WM tract connecting the posterior occipital lobe to the temporal lobe. This tract has been implicated not only in memory (Fuentemilla et al., 2009) but also in object recognition, linking objects to their lexical labels, and reading (Catani and Dawson, 2017). These results suggest that age-related declines in ILF structural connectivity may impair information processing in the MTL during naturalistic viewing.

An important question is why some regions such as the language network appear to be particularly resilient, while others, such as the FPCN, MTL, and mPFC are more sensitive to age-related declines in brain function. One factor could be the structural changes that are observed in the different brain regions with age. Although we have not looked at age-related declines in GM in this article, we did observe that the FC profile that was associated with reduced MTL synchrony was also related to a decline in WM microstructure in the right ILF. The preservation of synchrony in the language network occurs despite significant decline in GM volume in these regions (Campbell et al., 2016). These findings suggest that structural brain changes cannot fully explain these regional differences in sensitivity to age-related functional changes. We did observe a clear link between losses in synchrony and differences in FC with advancing age. This suggests that the reorganization of functional networks that occurs with advancing age across a different task states could be one of the factors contributing to the decline in synchrony. This reorganization is characterized by a reduction in the segregation between different functional systems, with the default mode and frontoparietal control networks showing particularly pronounced declines in within-network connectivity with age in previous studies (Andrews-Hanna et al., 2007; Chan et al., 2014; Geerligs et al., 2014, 2015a). However, we also observed that FC changes could not fully explain the age-related changes in synchrony. Other factors that influence the disparity between brain regions in their resilience to age may be their unique expression patterns of different neurotransmitter receptors (Zilles et al., 2015).

4.1. Limitations

The results of this study suggest that there are marked changes in information processing of naturalistic stimuli over the lifespan. While these naturalistic movie stimuli allow us to examine brain function in a context that is closer to real life than typical fMRI experiments, the downside of this approach is less experimental control. For example, we cannot exclude the possibility that there were differences over the lifespan in, for example, the gaze position of participants in particular scenes. However, we found that differences in auditory and visual network synchrony were less pronounced than differences in other regions and could not explain all of the age-related changes in the mPFC, MTL, and FPCN, suggesting that changes in viewing behavior are not the whole story. It is also not clear how dependent these results are on the movie stimulus that was used. The movie we used was selected based on previous studies showing that it yields some of the highest rates of synchrony across participants (possibly due to its captivating nature; Hasson et al., 2009). One concern with this movie is that it may be cohort specific, as it is a black and white movie, which was released in 1961. However, the correspondence between the age-sensitive regions we identified here and age-sensitive regions identified in task-based and resting-state paradigms (Fryer et al., 2015; Geerligs et al., 2015a; Samu et al., 2017) suggests that results may be robust. Given potential stimulus-specificity of the effects and the exploratory nature of the present study, a replication of our results is warranted.

Another important issue to consider in studies such as this is the impact of physiological or nonphysiological noise (e.g., head motion) on the outcome measures of interest. The intersubject synchrony measure should decline with the presence of noise, while FC measures could show increases as well as decreases depending on whether the cause of the noise was regionally specific (e.g., head motion) or more global (e.g., heart rate variability) (Geerligs et al., 2017; Power et al., 2017). We have taken great care to minimize such confounds both on the individual level and the group level, using ME-ICA denoising (Kundu et al., 2012), nuisance regression (Geerligs et al., 2017; Satterthwaite et al., 2013), group-level mean regression (Geerligs et al., 2017; Yan et al., 2013), and regression of head motion summary statistics to account for residual declines in synchrony due to age-related increases in head motion. The fact that we observe temporally (sliding window correlations) and spatially (FC results) separable patterns underlying the age-related differences synchrony in the 3 clusters of interest supports that the age-related changes we observe are not simply due to age-related increases in noise. Instead, they reflect age-related declines in specific functional brain systems, which vary in their expression based on the content of the movie.

One important caveat to note is that we did not have any direct behavioral outcome measures during the movie watching. Therefore, our interpretation of the age-related changes largely relies on reverse inference.

5. Conclusion

The present findings demonstrate the vulnerabilities and resilience of specific functional brain systems during movie watching, which is arguably more reflective of daily life experiences than standard experimental tasks. Our results suggest that brain regions involved in language processing remain intact with age, while areas involved in attentional control and memory show age-related declines. This is in line with deficits observed with

targeted behavioral experiments and suggests that these lab-based findings may also affect performance in real-world settings such as movie watching. Neural signals become increasingly individualistic as we age, and this could be associated with individual differences in functional brain organization and declines in WM integrity. One intriguing speculation is that this neural idiosyncrasy is indicative of a more individualistic experience of particular events as people age.

Acknowledgements

LG was supported by a Veni grant [451-16-013] from the Netherlands Organization for Scientific Research. KLC was supported by the Natural Sciences and Engineering Research Council of Canada (grant RGPIN-2017–03804 to KLC) and the Canada Research Chairs program. The Cambridge Centre for Ageing and Neuroscience (Cam-CAN) research was supported by the Biotechnology and Biological Sciences Research Council (grant number BB/H008217/1). The authors are grateful to the Cam-CAN respondents and their primary care teams in Cambridge for their participation in this study. The authors also thank colleagues at the MRC Cognition and Brain Sciences Unit MEG and MRI facilities for their assistance. The Cam-CAN corporate author consists of the project principal personnel: Lorraine K Tyler, Carol Brayne, Edward T Bullmore, Andrew C Calder, Rhodri Cusack, Tim Dalgleish, John Duncan, Richard N Henson, Fiona E Matthews, William D Marslen-Wilson, James B Rowe, and Meredith A Shafto. Research associates: Karen Campbell, Teresa Cheung, Simon Davis, Linda Geerligs, Rogier Kievit, Anna McCarrey, Abdur Mustafa, Darren Price, David Samu, Jason R Taylor, Matthias Treder, Kamen Tsvetanov, Janna van Belle, and Nitin Williams. Research assistants: Lauren Bates, Tina Emery, Sharon Erzinçlioglu, Andrew Gadie, Sofia Gerbase, Stanimira Georgieva, Claire Hanley, Beth Parkin, and David Troy. Affiliated personnel: Tibor Auer, Marta Correia, Lu Gao, Emma Green, and Rafael Henriques. Research interviewers: Jodie Allen, Gillian Amery, Liana Amunts, Anne Barcroft, Amanda Castle, Cheryl Dias, Jonathan Dowrick, Melissa Fair, Hayley Fisher, Anna Goulding, Adarsh Grewal, Geoff Hale, Andrew Hilton, Frances Johnson, Patricia Johnston, Thea Kavanagh-Williamson, Magdalena Kwasniewska, Alison McMinn, Kim Norman, Jessica Penrose, Fiona Roby, Diane Rowland, John Sargeant, Maggie Squire, Beth Stevens, Aldabra Stoddart, Cheryl Stone, Tracy Thompson, Ozlem Yazlik and administrative staff: Dan Barnes, Marie Dixon, Jaya Hillman, Joanne Mitchell, and Laura Villis.

Availability of data and analysis scripts: Access to the raw data used in this paper can be requested via https://camcan-archive.mrc-cbu.cam.ac.uk/dataaccess/. The pre-processed ROI time-courses, behavioural data and mean kurtosis values per WM tract, as well as documented analysis scripts that can be used to reproduce the results shown in this paper are available from the Research Data Repository of the Donders Institute (DI) for Brain, Cognition and Behaviour (http://hdl.handle.net/11633/di.dcc.DSC_2018.00013_064).

Appendix A. Supplementary data

Supplementary data associated with this article can be found, in the online version, at https://doi.org/10.1016/j.neurobiolaging.2018.07.025.

References

Aicher, C., Jacobs, A.Z., Clauset, A., 2013. Learning latent block structure in weighted networks. J. Complex Networks 3, 221–248.

Andrews-Hanna, J.R., Snyder, A.Z., Vincent, J.L., Lustig, C., Head, D., Raichle, M.E., Buckner, R.L., 2007. Disruption of large-scale brain systems in advanced aging. Neuron 56, 924–935.

Bailey, H.R., Zacks, J.M., Hambrick, D.Z., Zacks, R.T., Head, D., Kurby, C.A., Sargent, J.Q., 2013. Medial temporal lobe volume predicts elders' everyday memory. Psychol. Sci. 24, 1113–1122.

Baldassano, C., Chen, J., Zadbood, A., Pillow, J.W., Hasson, U., Norman, K.A., 2017. Discovering event structure in continuous narrative perception and memory. Neuron 95, 709–721.e5.

Ben-Amitay, S., Jones, D.K., Assaf, Y., 2012. Motion correction and registration of high b-value diffusion weighted images. Magn. Reson. Med. 67, 1694–1702.

Ben-Yakov, A., Eshel, N., Dudai, Y., 2013. Hippocampal immediate poststimulus activity in the encoding of consecutive naturalistic episodes. J. Exp. Psychol. Gen. 142, 1255–1263.

Benjamini, Y., Yekutieli, D., 2011. The control of the false discovery rate in multiple testing under dependency. Ann. Stat. 29, 1165–1188.

Benoit, R.G., Szpunar, K.K., Schacter, D.L., 2014. Ventromedial prefrontal cortex supports affective future simulation by integrating distributed knowledge. Proc. Natl. Acad. Sci. U. S. A. 111, 16550–16555.

Campbell, K.L., Grady, C.L., Ng, C., Hasher, L., 2012. Age differences in the frontoparietal cognitive control network: implications for distractibility. Neuropsychologia 50, 2212–2223.

Campbell, K.L., Shafto, M.A., Wright, P., Tsvetanov, K.A., Geerligs, L., Cusack, R., Cam-CAN, Tyler, L.K., 2015. Idiosyncratic responding during movie-watching predicted by age differences in attentional control. Neurobiol. Aging 36, 3045–3055.

Campbell, K.L., Davis, X.S.W., Geerligs, L., Mustafa, A., Tyler, L.K., 2016. Robust resilience of the frontotemporal syntax system to aging. J. Neurosci. 36, 5214–5227.

Catani, M., Dawson, M.S., 2017. Language processing, development and evolution. In: Conn's Translational Neuroscience. Elsevier, Cambridge, MA, pp. 679–692.

Cattell, R.B., Cattell, A.K.S., 1960. Handbook for the Individual or Group Culture Fair Intelligence Test. IPAT, Champaign, IL.

Chan, M.Y., Park, D.C., Savalia, N.K., Petersen, S.E., Wig, G.S., 2014. Decreased segregation of brain systems across the healthy adult lifespan. Proc. Natl. Acad. Sci. U. S. A. 111, E4997–E5006.

Craddock, R.C., James, G.A., Holtzheimer, P.E., Hu, X.P., Mayberg, H.S., 2012. A whole brain fMRI atlas generated via spatially constrained spectral clustering. Hum. Brain Mapp. 33, 1914–1928.

Craik, F.I.M., Byrd, M., 1982. Aging and cognitive deficits: the role of attentional resources. In: Craik, F.I.M., Trehub, S. (Eds.), Aging and Cognitive Processes. Plenum, New York, pp. 191–211.

Damoiseaux, J.S., Beckmann, C.F., Arigita, E.J.S., Barkhof, F., Scheltens, P., Stam, C.J., Smith, S.M., Rombouta, S.A., 2008. Reduced resting-state brain activity in the "default network" in normal aging. Cereb. Cortex. 18, 1856–1864.

Davis, S.W., Zhuang, J., Wright, P., Tyler, L.K., 2014. Age-related sensitivity to task-related modulation of language-processing networks. Neuropsychologia 63, 107–115.

Dmochowski, J.P., Sajda, P., Dias, J., Parra, L.C., 2012. Correlated components of ongoing EEG point to emotionally laden attention – a possible marker of engagement? Front. Hum. Neurosci. 6, 112.

Dorr, M., Martinetz, T., Gegenfurtner, K., Barth, E., 2010. Variability of eye movements when viewing dynamic natural scenes. J. Vis. 10, 28.

Falangola, M.F., Jensen, J.H., Babb, J.S., Hu, C., Castellanos, F.X., Di Martino, A., Ferris, S.H., Helpern, J.A., 2008. Age-related non-Gaussian diffusion patterns in the prefrontal brain. J. Magn. Reson. Imaging 28, 1345–1350.

Folstein, M.F., Folstein, S.E., McHugh, P.R., 1975. "Mini mental state". A practical method for grading the cognitive state of patients for the clinician. J. Psychiatr. Res. 12, 189–198.

Freund, A.M., Baltes, P.B., 1998. Selection, optimization, and compensation as strategies of life management: correlations with subjective indicators of successful aging. Psychol. Aging 13, 531–543.

Friedman, N.P., Miyake, A., 2004. The relations among inhibition and interference control functions: a latent-variable analysis. J. Exp. Psychol. Gen. 133, 101–135.

Fryer, S.L., Roach, B.J., Ford, J.M., Turner, J.A., van Erp, T.G.M., Voyvodic, J., Preda, A., Belger, A., Bustillo, J., O'Leary, D., Mueller, B.A., Lim, K.O., McEwen, S.C., Calhoun, V.D., Diaz, M., Glover, G., Greve, D., Wible, C.G., Vaidya, J., Potkin, S.G., Mathalon, D.H., 2015. Relating intrinsic low-frequency BOLD cortical oscillations to cognition in schizophrenia. Neuropsychopharmacology 40, 2705–2714.

Fuentemilla, L., Camara, E., Munte, T.F., Kramer, U.M., Cunillera, T., Marco-Pallares, J., Tempelmann, C., Rodriguez-Fornells, A., 2009. Individual differences in true and false memory retrieval are related to white matter brain microstructure. J. Neurosci. 29, 8698–8703.

Geerligs, L., Maurits, N.M., Renken, R.J., Lorist, M.M., 2014. Reduced specificity of functional connectivity in the aging brain during task performance. Hum. Brain Mapp. 35.

Geerligs, L., Renken, R.J., Saliasi, E., Maurits, N.M., Lorist, M.M., 2015a. A brain-wide study of age-related changes in functional connectivity. Cereb. Cortex. 25, 1987–1999.

Geerligs, L., Rubinov, M., Cam-CAN, Henson, R.N., 2015b. State and trait components of functional connectivity: individual differences vary with mental state. J. Neurosci. 35, 13949–13961.

Geerligs, L., Tsvetanov, K.A., Cam-CAN, Henson, R.N., 2017. Challenges in measuring individual differences in functional connectivity using fMRI: the case of healthy aging. Hum. Brain Mapp. 38, 4125–4156.

Gonzalez-Castillo, J., Panwar, P., Buchanan, L.C., Caballero-Gaudes, C., Handwerker, D.A., Jangraw, D.C., Zachariou, V., Inati, S., Roopchansingh, V., Derbyshire, J.A., Bandettini, P.A., 2016. Evaluation of multi-echo ICA denoising for task based fMRI studies: block designs, rapid event-related designs, and cardiac-gated fMRI. Neuroimage 141, 452–468.

Good, C.D., Johnsrude, I.S., Ashburner, J., Henson, R.N.A., Friston, K.J., Frackowiak, R.S.J., 2001. A voxel-based morphometric study of ageing in 465 normal adult human brains. Neuroimage 14, 21–36.

Grady, C.L., Protzner, A.B., Kovacevic, N., Strother, S.C., Afshin-Pour, B., Wojtowicz, M., Anderson, J.A.E., Churchill, N., McIntosh, A.R., 2010. A multivariate analysis of age-related differences in default mode and task-positive networks across multiple cognitive domains. Cereb. Cortex. 20, 1432–1447.

Hasson, U., Chen, J., Honey, C.J., 2015. Hierarchical process memory: memory as an integral component of information processing. Trends Cogn. Sci. 19, 304–313.

Hasson, U., Malach, R., Heeger, D.J., 2009. Reliability of cortical activity during natural stimulation. Trends Cogn. Sci. 14, 40–48.

Hasson, U., Nir, Y., Levy, I., Fuhrmann, G., Malach, R., 2004. Intersubject synchronization of cortical activity during natural vision. Science 303, 1634–1640.

Hasson, U., Yang, E., Vallines, I., Heeger, D., Rubin, N., 2008. A hierarchy of temporal receptive windows in human cortex. J. Neurosci. 28, 2539–2550.

Hua, X., Leow, A.D., Parikshak, N., Lee, S., Chiang, M.-C., Toga, A.W., Jack, C.R., Weiner, M.W., Thompson, P.M., 2008. Tensor-based morphometry as a neuroimaging biomarker for Alzheimer's disease: an MRI study of 676 AD, MCI, and normal subjects. Neuroimage 43, 458–469.

Jeffreys, H., 1961. The Theory of Probability. Oxford University Press, Oxford.

Jenkinson, M., Bannister, P., Brady, M., Smith, S., 2002. Improved optimization for the robust and accurate linear registration and motion correction of brain images. Neuroimage 17, 825–841.

Krall, S.C., Rottschy, C., Oberwelland, E., Bzdok, D., Fox, P.T., Eickhoff, S.B., Fink, G.R., Konrad, K., 2015. The role of the right temporoparietal junction in attention and social interaction as revealed by ALE meta-analysis. Brain Struct. Funct. 220, 587–604.

Kundu, P., Inati, S.J., Evans, J.W., Luh, W.-M., Bandettini, P.A., 2012. Differentiating BOLD and non-BOLD signals in fMRI time series using multi-echo EPI. Neuroimage 60, 1759–1770.

Kurby, C.A., Asiala, L.K.E., Mills, S.R., 2014. Aging and the segmentation of narrative film. Aging Neuropsychol. Cogn. 21, 444–463.

Kurby, C.A., Zacks, J.M., 2011. Age differences in the perception of hierarchical structure in events. Mem. Cognit. 39, 75–91.

Mather, M., Carstensen, L.L., 2005. Aging and motivated cognition: the positivity effect in attention and memory. Trends Cogn. Sci. 9, 496–502.

May, C.P., Rahhal, T., Berry, E.M., Leighton, E.A., 2005. Aging, source memory, and emotion. Psychol. Aging 20, 571–578.

Moscovitch, M., Cabeza, R., Winocur, G., Nadel, L., 2016. Episodic memory and beyond: the hippocampus and neocortex in transformation. Annu. Rev. Psychol. 67, 105–134.

Naci, L., Cusack, R., Anello, M., Owen, A.M., 2014. A common neural code for similar conscious experiences in different individuals. Proc. Natl. Acad. Sci. U. S. A. 111, 14277–14282.

Neto Henriques, R.N., Correia, M.M., 2015. Reducing Inter and Intra-Volume Instabilities on Diffusion-Weighted Data for Ageing Studies I. OHBM, Geneva, Switzerland, p. 22924.

Oren, N., Shapira-Lichter, I., Lerner, Y., Tarrasch, R., Hendler, T., Giladi, N., Ash, E.L., 2017. Schema benefit vs. proactive interference: contradicting behavioral outcomes and coexisting neural patterns. Neuroimage 158, 271–281.

Power, J., Plitt, M., Kundu, P., Bandettini, P., Martin, A., 2015. Analyses of Motion Artifact Before and After Multi-Echo ICA Denoising. OHBM, Honolulu, HI.

Power, J.D., Plitt, M., Laumann, T.O., Martin, A., 2017. Sources and implications of whole-brain fMRI signals in humans. Neuroimage 146, 609–625.

Preston, A.R., Eichenbaum, H., 2013. Interplay of hippocampus and prefrontal cortex in memory. Curr. Biol. 23, R764–R773.

Ramscar, M., Sun, C.C., Hendrix, P., Baayen, H., 2017. The mismeasurement of mind: life-span changes in paired-associate-learning scores reflect the "cost" of learning, not cognitive decline. Psychol. Sci. 28, 1171–1179.

Samu, D., Campbell, K.L., Tsvetanov, K.A., Shafto, M.A., Cam-CAN, Tyler, L.K., 2017. Preserved cognitive functions with age are determined by domain-dependent shifts in network responsivity. Nat. Commun. 8, 14743.

Satterthwaite, T.D., Elliott, M.A., Gerraty, R.T., Ruparel, K., Loughead, J., Calkins, M.E., Eickhoff, S.B., Hakonarson, H., Gur, R.C., Gur, R.E., Wolf, D.H., 2013. An improved framework for confound regression and filtering for control of motion artifact in the preprocessing of resting-state functional connectivity data. Neuroimage 64, 240–256.

Schacter, D.L., Addis, D.R., Hassabis, D., Martin, V.C., Spreng, R.N., Szpunar, K.K., 2012. The future of memory: remembering, imagining, and the brain. Neuron 76, 677–694.

Shafto, M.A., Tyler, L.K., Dixon, M., Taylor, J.R., Rowe, J.B., Cusack, R., Calder, A.J., Marslen-Wilson, W.D., Duncan, J., Dalgleish, T., Henson, R.N., Brayne, C., Cam-CAN, Matthews, F.E., 2014. The Cambridge Centre for Ageing and Neuroscience (Cam-CAN) study protocol: a cross-sectional, lifespan, multidisciplinary examination of healthy cognitive ageing. BMC Neurol. 14, 204.

Shen, X., Finn, E.S., Scheinost, D., Rosenberg, M.D., Chun, M.M., Papademetris, X., Constable, R.T., 2017. Using connectome-based predictive modeling to predict individual behavior from brain connectivity. Nat. Protoc. 12, 506–518.

Shulman, G.L., Corbetta, M., 2012. Two attentional networks: identification and function within a larger cognitive architecture. In: Posner, M.I. (Ed.), Cognitive Neuroscience of Attention. The Guilford Press, New York, pp. 113–128.

Simony, E., Honey, C.J., Chen, J., Lositsky, O., Yeshurun, Y., Wiesel, A., Hasson, U., 2016. Dynamic reconfiguration of the default mode network during narrative comprehension. Nat. Commun. 7, 12141.

Taylor, J.R., Williams, N., Cusack, R., Auer, T., Shafto, M.a., Dixon, M., Tyler, L.K., Cam-CAN, Henson, R.N., 2017. The Cambridge Centre for Ageing and Neuroscience (Cam-CAN) data repository: structural and functional MRI, MEG, and cognitive data from a cross-sectional adult lifespan sample. Neuroimage 144, 262–269.

Turner, G.R., Spreng, R.N., 2015. Prefrontal engagement and reduced default network suppression co-occur and are dynamically coupled in older adults: the default–executive coupling hypothesis of aging. J. Cogn. Neurosci. 27, 2462–2476.

Tyler, L.K., Wright, P., Randall, B., Marslen-Wilson, W.D., Stamatakis, E.A., 2010. Reorganization of syntactic processing following left-hemisphere brain damage: does right-hemisphere activity preserve function? Brain 133, 3396–3408.

Umanath, S., Marsh, E.J., 2014. Understanding how prior knowledge influences memory in older adults. Perspect. Psychol. Sci. 9, 408–426.

van Kesteren, M.T.R., Fernandez, G., Norris, D.G., Hermans, E.J., 2010. Persistent schema-dependent hippocampal-neocortical connectivity during memory encoding and postencoding rest in humans. Proc. Natl. Acad. Sci. U. S. A. 107, 7550–7555.

Van Kesteren, M.T.R., Ruiter, D.J., Fernández, G., Henson, R.N., 2012. How schema and novelty augment memory formation. Trends Neurosci. 35, 211–219.

Vincent, J.L., Kahn, I., Snyder, A.Z., Raichle, M.E., Buckner, R.L., 2008. Evidence for a frontoparietal control system revealed by intrinsic functional connectivity. J. Neurophysiol. 100, 3328–3342.

Wechsler, D., 1999. Wechsler Memory Scale, Third ed. Harcourt Assessment, London.

Wetzels, R., Wagenmakers, E.-J., 2012. A default Bayesian hypothesis test for correlations and partial correlations. Psychon. Bull. Rev. 19, 1057–1064.

Winecoff, A., Clithero, J.A., Carter, R.M., Bergman, S.R., Wang, L., Huettel, S.A., 2013. Ventromedial prefrontal cortex encodes emotional value. J. Neurosci. 33, 11032–11039.

Yan, C.G., Craddock, R.C., Zuo, X.N., Zang, Y.F., Milham, M.P., 2013. Standardizing the intrinsic brain: towards robust measurement of inter-individual variation in 1000 functional connectomes. Neuroimage 80, 246–262.

Zacks, J.M., Speer, N.K., Swallow, K.M., Maley, C.J., 2010. The brain's cutting-room floor : segmentation of narrative cinema. Front. Aging Neurosci. 4.

Zacks, J.M., Speer, N.K., Vettel, J.M., Jacoby, L.L., 2006. Event understanding and memory in healthy aging and dementia of the Alzheimer type. Psychol. Aging 21, 466–482.

Zhang, S., Li, C., shan, R., 2012. Functional connectivity mapping of the human precuneus by resting state fMRI. Neuroimage 59, 3548–3562.

Zilles, K., Bacha-Trams, M., Palomero-Gallagher, N., Amunts, K., Friederici, A.D., 2015. Common molecular basis of the sentence comprehension network revealed by neurotransmitter receptor fingerprints. Cortex 63, 79–89.

Zimmerman, S., Hasher, L., Goldstein, D., 2011. Cognitive ageing: a positive perspective. In: Kapur, N. (Ed.), The Paradoxical Brain. Cambridge University Press, Cambridge, pp. 130–150.